Second-order bosonic Kadanoff-Baym equations for plasmon-accompanied optical absorption

Michael Schüler, Yaroslav Pavlyukh
Martin Luther University Halle-Wittenberg, 06099 Halle (Saale), Germany
E-mail: michael.schueler@physik.uni-halle.de

Abstract. The availability of ultra-short and strong light sources opens the door for a variety of new experiments such as transient absorption, where optical properties of systems can be studied in extreme nonequilibrium situations. The nonequilibrium Green's function formalism is an efficient approach to investigate these processes theoretically. Here we apply the method to the light-matter interaction of the magnesium 2p core level accompanied by electron-plasmon interaction due to collective excitations in the conduction band. The plasmons are described as massive bosonic quasi-particle excitations, leading to a second-order equations of motion, requiring a new approach for their propagation.

1. Introduction

Electronic correlations are manifest in a number of spectroscopic experiments. Photoemission [1, 2] and, in particular, double photoemission [3, 4, 5], photoabsorption or electron-energy loss spectroscopy (EELS) represent some of the most direct approaches. Here we exemplary focus on photoabsorption. The central quantity hereby is the density-density response function χ, which is a genuine two-body quantity and thus captures electron (or hole) pair correlations. Computing χ is typically an involved task. Depending on the system at hand, few approaches are suitable. For small systems, full (or truncated) CI methods deliver accurate many-body properties including the complete particle-hole (*e*-*h*) spectrum. This route becomes inaccessible with growing system size, such that approximative schemes are invoked. One of the most employed approach is many-body perturbation theory (MBPT), where χ is obtained from the four-point *e*-*h* propagator L [6, 7]. In turn, L is the solution to the Bethe-Salpeter equation (BSE). In combination with the GW approximation [8], the BSE approach has been widely applied to molecules, clusters and solids [9, 10, 11, 12, 13, 14].

An alternative route to access χ is to directly use linear response, as the variation of any one-body observable (e. g. the dipole moment) upon applying a weak perturbation potential $\delta\varphi$ is proportional to the convolution of χ with $\delta\varphi$. Hence, carrying out real-time propagation of the system is required in this framework. One important method solving this task is time-dependent density-functional theory (TDDFT) [15]. Its advantage lies in relatively low computation cost, which allows for efficiently computing linear response properties of molecules up to larger clusters [16, 17, 18, 19].

On the other hand, TDDFT is currently only available within the adiabatic approximation and thus lacks memory effects. The nonequilibrium Green's function (NEGF) formalism is a natural tool for accounting both correlation and memory effects. The equations of motion (EOM) for the Green's functions (GFs), the Kadanoff-Baym equations (KBEs), allow hereby taking the MBPT to the time domain [20, 21, 22], providing important assessment on advanced approximation schemes [23, 24, 25]. A time-dependent approach beyond the adiabatic approximation becomes increasingly important in view

of the impressive advances in generating attosecond laser pulses [26, 27, 28], providing insights in transient electron dynamics in systems ranging from atoms to solids [29, 30, 31]. Pump-probe setups using these light sources hence are able to deliver *transient* optical properties such as transient absorption [29, 32, 33, 34].

In this contribution we study the KBE nonequilibrium dynamics of electrons coupled to bosonic quasi-particle excitations such as phonons, vibrons, quantized photons or plasmons. One prototypical model in this regard is the s-model originally proposed by Lundqvist [35] and solved by Langreth [36]. It was introduced to describe photoemission from a deep core states accompanied by the creation of a plasmon [37]. This inelastic process is reflected in a series of plasmon satellites (PSs) on the left- and side of the quasi-particle peak (QP) in the spectral function. Such electron-boson model follows, e. g., from plasmon-pole approximation for the screened interaction W [8], electron-phonon (or electron-vibron) interaction [38, 39, 40, 41, 42]. Although we focus on electron-plasmon interaction here, the methodology presented here is applicable to other electron-boson systems, as well. Hence, related methods such as molecular pump-probe spectroscopy [43, 44, 45, 46, 47] lie within the scope of our approach.

We present the KBEs for the relevant correlators of coupled electron-boson system in the framework of the MBPT (sec. 2), going beyond the standard frozen-boson approach [48, 49]. We apply our theory to the transient absorption of the Mg 2p core level accompanied by plasmon excitations in the conduction band (sec. 3).

2. Hamiltonian and equations of motion

We consider an electronic system with single-particle (SP) energies ϵ_i with corresponding fermionic annihilation operators $\hat{c}_i$. The electrons are assumed to interact with a single boson mode with energy Ω and bosonic annihilation operator $\hat{b}$. The equivalent coordinate-momentum representation of the bosons, that is

$$\hat{Q} = \frac{1}{\sqrt{2}}\left(\hat{b} + \hat{b}^\dagger\right), \quad \hat{P} = -\frac{\mathrm{i}}{\sqrt{2}}\left(\hat{b} - \hat{b}^\dagger\right) \tag{1}$$

will be used in what follows. A generalization to the multi-boson case is straightforward and will be presented elsewhere. Besides the effective interaction mediated by the electron-boson coupling, no further electron-electron interaction is accounted for. The total Hamiltonian describing the system in equilibrium is taken as

$$\hat{H}_0 = \hat{H}_{\mathrm{el}} + \hat{H}_{\mathrm{el-bos}} + \hat{H}_{\mathrm{bos}}\,, \tag{2}$$

where

$$\hat{H}_{\mathrm{el}} = \sum_i \epsilon_i \hat{c}_i^\dagger \hat{c}_i\,, \quad \hat{H}_{\mathrm{bos}} = \frac{\Omega}{2}\left(\hat{P}^2 + \hat{Q}^2\right) \tag{3}$$

are the Hamiltonians describing the individual subsystems. The coupling Hamiltonian is adopted to the deep core-level scenario:

$$\hat{H}_{\mathrm{el-bos}} = \sum_i \Gamma_i \hat{c}_i \hat{c}_i^\dagger \hat{Q}\,. \tag{4}$$

Note that generalizing to the more general matrix case $\Gamma_i \to \Gamma_{ij}$ does not cause any technical difficulties. Light-matter interaction targeting the electrons is taken into account by

$$\hat{H}_{\mathrm{el-L}}(t) = \sum_{ij} F_{ij}(t)\hat{c}_i^\dagger \hat{c}_j + \mathrm{h.c.}\,, \tag{5}$$

Besides the usual one-electron GF $G_{ij}(t,t') = -\mathrm{i}\langle \mathcal{T}\hat{c}_i(t)\hat{c}_j^\dagger(t')\rangle$, the suitable counterpart describing bosonic properties is the coordinate-coordinate fluctuation correlator

$$D(t,t') = -\mathrm{i}\left[\langle \mathcal{T}\hat{Q}(t)\hat{Q}(t')\rangle - \langle\hat{Q}(t)\rangle\langle\hat{Q}(t')\rangle\right]\,. \tag{6}$$

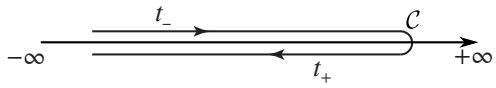

Figure 1. The real contour C, running from $-\infty$ to some finite time and back to $-\infty$. The subscripts + (−) of a contour argument t that it belongs to lower (upper) branch of the contour.

Time arguments lie on the Keldysh contour $t = t_\pm \in C$ shown in fig. 1 (contour ordering operator $\mathcal{T}$).

The derivation of the coupled EOM for $G_{ij}(t,t')$ and $D(t,t')$ follows from the standard Heisenberg EOM. It should be noted though that applying the derivative $\mathrm{i}\partial_t$ to $D(t,t')$ is not yielding a closed equation, as $\partial_t \hat{Q}(t) = \Omega \hat{P}(t)$. Applying the derivative again on the other hand one obtains

$$\partial_t^2 \hat{Q}(t) = -\Omega^2 \hat{Q}(t) - \sum_i \Gamma_i \hat{c}_i(t) \hat{c}_i^\dagger(t) \,,$$

which has the form of a driven harmonic oscillator equation. Replacing the occurrence of higher-order correlators by respective convolutions with corresponding self-energies, the EOM for both the electron and the boson GFs attains the form [1]

$$\mathrm{i}\partial_t G_{ij}(t,t') = \delta_{ij}\delta(t-t') + \sum_k h_{ik}^{\mathrm{MF}}(t) G_{kj}(t,t') + \sum_k \int_C \mathrm{d}t''\, \Sigma_{ik}(t,t'') G_{kj}(t'',t') \,, \tag{7}$$

$$-\frac{1}{\Omega}\left(\partial_t^2 + \Omega^2\right) D(t,t') = \delta(t-t') + \int_C \mathrm{d}t''\, \Pi(t,t'') D(t'',t') \,. \tag{8}$$

In the context of electron-phonon interaction, the lowest-order approximations to electron self-energy $\Sigma_{ij}(t,t')$ and the boson self-energy $\Pi(t,t')$ is known as the self-consistent Born approximation [39, 40, 50, 51]. Besides the mean-field term

$$h_{ij}^{\mathrm{MF}}(t) = \epsilon_i \delta_{ij} + F_{ij}(t) - \Gamma_i \delta_{ij} \langle \hat{Q}(t) \rangle \,, \tag{9}$$

one obtains

$$\Sigma_{ij}^{(2)}(t,t') = \mathrm{i}\Gamma_i \Gamma_j G_{ij}(t,t') D(t,t') \,, \tag{10}$$

$$\Pi^{(2)}(t,t') = -\mathrm{i} \sum_{ij} \Gamma_i \Gamma_j G_{ij}(t,t') G_{ji}(t',t) \tag{11}$$

as second-order (in electron-boson interaction) self-energies. Eq. (10)–(11) can be paralleled with the GW approximation to Hedin's equations [7] — $\Gamma_i \Gamma_j D(t,t')$ hereby plays the role of the dynamical part of the screened interaction W. In case W is dominated by one plasmonic excitation, the plasmon-pole approximation applies and allows for reducing a system of interacting electrons to the electron-boson model investigated here. Therefore, we will term eq. (10)–(11) as GW approximation in what follows. Analogously, the GW_0 approximation refers to ignoring $\Pi^{(2)}(t,t')$, such that the boson correlator $D(t,t')$ is entirely non-interacting.

Importantly, the bosonic dynamics is not only captured by the coordinate-coordinate correlator $D(t,t')$ (which contains information on the fluctuations of $\hat{Q}$), but by the boson amplitude $\langle \hat{Q}(t) \rangle$, as well. This is quite distinct from electronic propagators. Because of the explicit appearance of $\langle \hat{Q}(t) \rangle$, a respective EOM needs to be formulated:

$$-\frac{1}{\Omega}\left(\frac{\mathrm{d}^2}{\mathrm{d}t^2} + \Omega^2\right) \langle \hat{Q}(t) \rangle = \mathrm{i} \sum_i \Gamma_i G_{ii}(t^+,t) \,, \tag{12}$$

[1] A rigorous derivation can be done employing a source-field approach similar to Hedin's equations [6] and is the scope of future work.

where t^+ is (with respect to the contour ordering) infinitesimally larger that t.

Inserting the second-order approximation to the self-energy, eq. (10)–(11), eq. (7)–(8) in combination with eq. (9)–(12) leads to a self-consistent set of equations. The solution strategy relies, as usual, on the projection of the contour arguments onto observables times. The specific arrangements $G_{ij}(t_+, t'_-) \equiv G^{>}_{ij}(t, t')$ ($G_{ij}(t_-, t'_+) \equiv G^{<}_{ij}(t, t')$) are known as the greater (lesser) GF ($D^{\gtrless}$ is defined analogously). Note that the time arguments of $G^{\gtrless}_{ij}$ refer to real, observables times now. By employing the Langreth rules [22, 7], eq. (7)–(8) is then transformed into the KBEs, which are solved with a method similar to ref. [52]. Appropriate modifications for treating the second-order KBE for the boson propagators are incorporated by replacing the Heun method (first order) by Numerov's method (second order).

Note that the contour fig. 1 lacks the imaginary track which required to account for a correlated initial state. Hence, we apply the method of adiabatic switching [22], allowing for working with lesser/greater GFs only.

3. Transient absorption of Mg 2p core level

As a proof-of-principle we apply the theory outlined in sec. 2 to core-level photoabsorption. For concreteness, we consider the transition from the magnesium 2p core level to the conduction band. We construct the electronic part of eq. (2) comprising two electronic levels $|2\mathrm{p}\rangle$ and an excited state $|f\rangle$ located just above the Fermi energy ϵ_F. In principle, a continuum of Bloch states needs to be accounted for when describing photoabsorption, describing (i) transitions within the conduction band including plasmon excitation, and (ii) transitions from the core level to states above the vacuum level (see fig. 2). Both types of processes are reflected in a, possibly large, background signal. We are however interested in the onset attributed to the plasmon satellites originating from the excitation of the core state. In the pump-probe setup detailed below, the pump pulse can be tuned to resonantly create a core hole. The processes (i) and (ii) will thus hardly be affected. Therefore, the mostly static background can be removed. The electron-boson model eq. (2) that lacks this background is then well suited for describing the remaining plasmonic features. Furthermore, we take the continuum of accessible states into account in a approximate fashion by coupling the $|f\rangle$ to an environment. This is accomplished by adding an embedding self-energy $\Sigma^{\mathrm{em},\gtrless}_f(t, t') = \Sigma^{\mathrm{em},\gtrless}_f(t - t')$ to eq. (10). For simplicity, we keep it within the wide-band limit approximation (WBLA) [7], defined by

$$\Sigma^{\mathrm{em},<}_f(t) = \mathrm{i}\,\Gamma_\mathrm{em} \int_{-\infty}^{\epsilon_\mathrm{F}} \frac{\mathrm{d}\omega}{2\pi} e^{-\mathrm{i}\omega t} e^{\eta(\omega-\epsilon_\mathrm{F})}\,, \quad \Sigma^{\mathrm{em},>}_f(t) = -\mathrm{i}\,\Gamma_\mathrm{em} \int_{\epsilon_\mathrm{F}}^{\infty} \frac{\mathrm{d}\omega}{2\pi} e^{-\mathrm{i}\omega t} e^{-\eta(\omega-\epsilon_\mathrm{F})} \tag{13}$$

where $\eta > 0$ is a regularization constant (we set $\eta = 0.01$). The embedding coupling constant is set to $\Gamma_\mathrm{em} = 3$ eV, leading to a broadening of $|f\rangle$ comparable to the band width of accessible states below the vacuum energy. The parameters entering the Hamiltonian are estimated in line with experiments [53, 54]. We take $\epsilon_{2\mathrm{p}} = -50$ eV, $\epsilon_f = -3.68$ eV (see fig. 2(a)). Only after the electron was excited from the core state it interacts with plasmons. Hence Γ_f can be assumed as zero, while we take $\Gamma_{2\mathrm{p}} = 5$ eV. The plasmons, in turn, originate from transitions around the Fermi level. They are treated within the small-momentum limit, i. e. the plasmon dispersion is ignored, and only a single plasmon mode $\Omega \simeq 10$ eV is incorporated (see fig. 2(a)). Solving the KBEs in equilibrium yields a spectral function of the core level with a strength of the first PS comparable to what has been observed [53].

In order to investigate the excited-state properties within optical absorption, we apply specific fields. We choose $F_{ij}(t) = f(t)m_{ij}$, where $m_{2\mathrm{p},2\mathrm{p}} = m_{f,f} = 0$ and $m_{2\mathrm{p},f} = m_{f,2\mathrm{p}}$ defines the dipole operator of the system. According to linear response theory [55], the change of the density matrix ρ_{ij} upon applying a weak field $F_{ij}(t)$ is determined by the retarded response function $\chi^{\mathrm{R}}_{ijkl}(t, t')$:

$$\delta\rho_{ij}(t) = \sum_{kl} \int_0^\infty \mathrm{d}t'\, \chi^{\mathrm{R}}_{ijkl}(t, t') F_{kl}(t')\,. \tag{14}$$

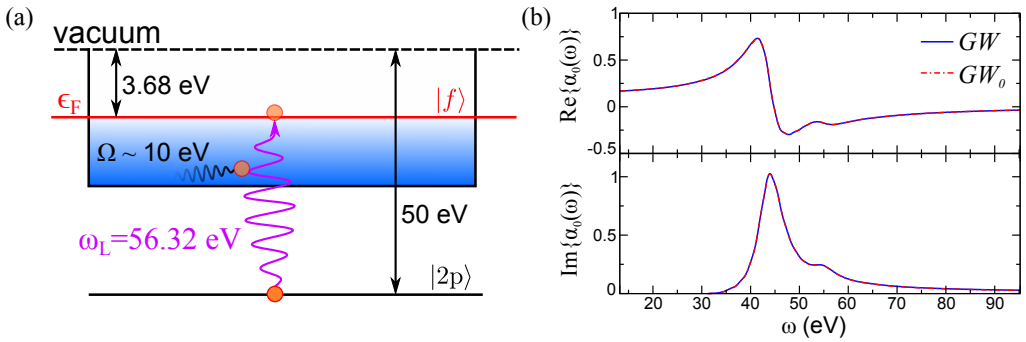

Figure 2. (a) Sketch of model system for describing absorption from the magnesium 2p core level ($|2p\rangle$) to an unoccupied state right above the Fermi level ϵ_F ($|f\rangle$) accompanied by plasmon excitations in the conduction band. (b) Equilibrium polarizability $\alpha_0(\omega)$ in both the GW and the GW_0 approximation, computed by the time-propagation method.

Hence, the dipole response of the system is governed by the polarizability

$$\alpha(t,t') = \sum_{ijkl} m_{ji}\chi^{\mathrm{R}}_{ijkl}(t,t')m_{kl} \,.$$

In equilibrium, $\alpha(t,t') = \alpha_0(t-t')$ depends on the time difference only, such that Fourier transformation with respect to $t-t'$ is possible. The convolution eq. (14) is thus turned into multiplication in frequency space. The induced dipole is then just given by $\delta M(\omega) = \alpha_0(\omega)f(\omega)$. The special case $f(t) = f_0\delta(t)$ directly allows for computing $\alpha_0(\omega) = \delta M(\omega)/f_0$. As usual, refractive properties are encoded in the real part, whereas the imaginary part contains information on the absorbed photons.

The equilibrium polarization $\alpha_0(\omega)$ is shown in fig. 2(b), calculated in both the GW as well as in the GW_0 approximations. The results for the two cases are identical — a behavior that is to be expected as the boson self-energy eq. (11) exactly vanishes if the 2p level is fully occupied in the initial state. Therefore, the GW_0 approximation is well suited for studying (general) electron-boson systems close to equilibrium, a fact that is often utilized for simplifying the treatment of electron-phonon interaction [38]. The main feature of the absorption spectrum $\mathrm{Im}\{\alpha_0(\omega)\}$ is, besides the strong QP peak, a PS (further satellites are existing but rapidly loosing spectral weight) separated by $+\Omega$ from the QP peak (denoted by PS^+). Hence, the absorption spectra resembles the (inverted and shifted) spectral function that is broadened by the environmental coupling of the $|f\rangle$ state.

This picture changes substantially in an excited-state scenario, where the plasmonic dynamics due to the electronic excitation can no longer be ignored. The optical properties encoded in the polarizability of this excited system can, depending on the pulse strength, be very different from fig. 2(b). Experimentally, this dynamical scenario can be studied using transient absorption: a short (but spectrally confined) pulse resonantly induces excitations, whereas a second (spectrally broad) pulse probes the system [29, 32, 33, 34]. In order to reflect this setup we modify the driving field $f(t) = f_{\mathrm{pump}}(t) + f_{\mathrm{probe}}(t)$; $f_{\mathrm{probe}}(t) = f_0\delta(t-\tau)$ is the probe pulse and $f_{\mathrm{pump}}(t) = f_{p,0}\sin(\omega_L t)\sin^2(\pi t/T_p)$ for $0 < t < T_p$ and $f_{\mathrm{pump}}(t) = 0$ otherwise denotes the pump pulse. Here, T_p denotes the pulse duration and ω_L the central frequency. The latter is tuned to $\omega_L = \epsilon_f - \epsilon_{2p}$. The pulse duration is fixed at $T_p = 0.5$ fs, it comprises 5-cycles, but still has a well defined energy. The time τ denotes the time delay between pump and probe; $\tau < 0$ means the probe precedes the excitation, while for $0 < \tau < T_p$ pump and probe overlap and $\tau > T_p$ corresponds to probing the system after the pump pulse has been switched off.

The time-dependent dipole moment $\delta M(t)$ has now two contributions: $\delta M(t) = \delta M_{\mathrm{pump}}(t) + \delta M_{\mathrm{probe}}(t)$. As the pump pules might be strong, linear response theory does not apply here. However, choosing the probe amplitude f_0 sufficiently small allows for characterizing the probe contribution to the total dipole

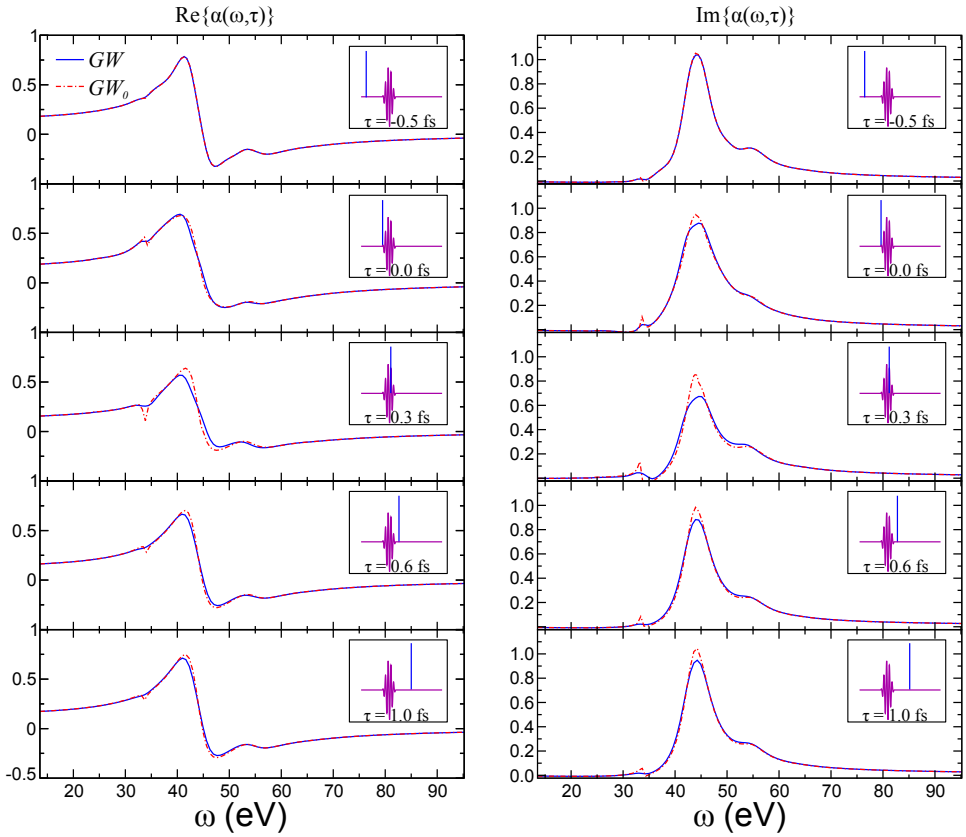

Figure 3. Transient refraction (left panel) and absorption (right) spectra for the GW (solid blue) and GW_0 (red dot-dashed line) approximation. The inset sketches the temporal arrangement of pump (amplitude $f_{p,0} = 0.1$ a. u.) and probe pulses.

moment by $\delta M_{\text{probe}}(t) = f_0 \alpha(t, \tau)$. Fourier transforming,

$$\alpha(\omega, \tau) = \frac{1}{f_0} \delta M_{\text{probe}}(\omega) = \int_{-\infty}^{\infty} \mathrm{d}t \, e^{\mathrm{i}\omega t} \delta M_{\text{probe}}(t) = \int_{-\infty}^{\infty} \mathrm{d}t \, e^{\mathrm{i}\omega t} \left[\delta M(t) - \delta M_{\text{pump}}(t) \right] , \tag{15}$$

yields the frequency- and delay-dependent polarizability $\alpha(\omega, \tau)$. As performing the time propagation delivers the total dipole $\delta M(t)$ only, two calculations have to be performed for each τ: one with $f_0 = 0$ and one with finite f_0 in order to individually determine the difference in the square brackets in eq. (15).

In fig. 3 we present transient absorption spectra $\alpha(\omega, \tau)$ for a weak pump pulse $f_{p,0} = 3$ eV, corresponding to a depopulation of $|2\mathrm{p}\rangle$ by 0.15. For $\tau < 0$ the behavior of both refraction and absorption are close to the equilibrium case. Increasing τ we observe the transient formation of a second PS located at the left of the QP peak (let us denote it by PS^-) – this is due to the non-zero plasmon occupation resulting from the pump pulse. This picture is consistent with the equilibrium case (no pulses applied), where the spectral function computed with nonzero (but fixed) plasmon occupation displays a PS^- peak, as well (fig. 4(a)). For overlapping pump and probe pulse ($\tau = 0$) the QP peak is suppressed, as finite population of $|f\rangle$ decreases the excitation probability. The QP gains spectral weight again with increasing τ, as the population of $|f\rangle$ vanishes due to the environmental coupling. Generally, the GW and GW_0 approximations agree well also in the transient case, except when pump and probe pulse overlap. This is expected as the system is in a nonequilibrium state due to the laser driving. Furthermore, the GW_0 approximation predicts a spiky PS^- at $\omega \simeq 33$ eV, whereas PS^- is smooth within the full GW approximation.

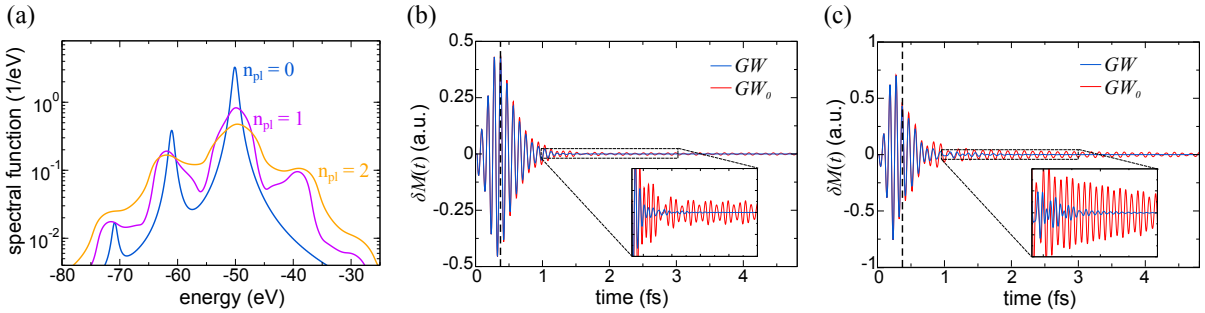

Figure 4. (a) Spectral function of the system in equilibrium with fixed plasmon occupation number $n_{\mathrm{pl}} = 0, 1, 2$. (b) Induced dipole oscillations $\delta M(t)$ for $f_{p,0} = 0.1$ a. u., and (c) $f_{p,0} = 0.3$ a. u.; the horizontal dashed black line indicates the time $t = \tau = 0.3$ fs. when the δ-kick is applied.

This is an indication of different damping behavior of $\delta M(t)$ in the two cases: because the full time dependence enters the Fourier transformation in eq. (15), relaxation and dephasing play an important role. For instance, applying the probe pulse long after the system has been excited ($\tau \to \infty$) is only sensitive to the new steady state, while probing immediately after provides insight in the equilibration. Similarly, $\tau \to -\infty$ yields the equilibrium spectrum, whereas $\alpha(\omega, \tau)$ for finite $\tau < 0$ is still influenced by the probe pulse. How rapidly the limit $\tau \to \pm\infty$ is reached depends on the damping strength. For our system, $|f\rangle$ is directly damped by the embedding self-energy, while $|2\mathrm{p}\rangle$ experiences damping by correlation due to the electron-plasmon interaction. Additional tests show that $\delta M(t)$ indeed is quickly damped within the GW approximation, while a small oscillation amplitude associated to PS^- remains when employing the GW_0 approximation (see fig. 4(b)). The formation of PS^- hereby is only due to the (first-order) mean-field contribution to eq. (9), meaning that the boson coordinate $\langle \hat{Q}(t) \rangle$ oscillates, but its fluctuation described by $D(t, t')$ is unaffected. Due to the self-energy, energy is transfered from the electronic subsystem to the plasmon subsystem, leading to damping of the electronic excitation. In the GW_0 approximation however, an infinite amount of energy can, in principle, flow into the bosonic degrees of freedom, at variance to the GW approximation.

We proceed by increasing the pump pulse strength to $f_{p,0} = 0.3$ a. u., lowering the occupation of the core level down to 0.17 after the pulse. The results for the dynamical polarizability are depicted in fig. 5. This almost perfect population inversion simulates a strong deviation from the equilibrium. Indeed, increasing τ until pump and probe pulse overlap, $\alpha(\omega, \tau)$ becomes mostly negative – the system does not absorbs photons, but predominantly emits light, mostly at the energy of the QP and PS^- peaks. Hence, the down-conversion to smaller light frequencies occurs in the system. This is a signature of nonlinearities and cannot be observed if the two subsystems are not coupled. For larger τ, the relaxation of the $|f\rangle$ state allows for transferring population to this state again. Since $|2\mathrm{p}\rangle$ is almost empty, the optical response is however strongly suppressed. Again we realize that the GW_0 approximation delivers an overall good description, apart from strongly nonequilibrium situations. This is particularly apparent for $\tau = 0.6$ fs, where significant deviations occur. Since the PS^- peak is pertinent to the scenario where the bosonic mode is in nonequilibrium it is poorly described by the GW_0 approximation, as well (similar to fig. 3). Fig. 4(c) shows the dipole $\delta M(t)$ for both approximations. It shows that GW_0 propagation is weaker damped which can be traced back to the form of the imaginary part of the self-energy in the frequency domain. In this case there are no features that would lead to an efficient damping of PS^- state.

4. Conclusions

We studied the equilibrium and transient refraction and absorption properties of a model system describing electron-plasmon interaction of core levels in metals. The plasmon mode was characterized by the collective coordinate $\langle Q(t) \rangle$ and the coordinate-coordinate fluctuation correlator $D(t, t')$. We

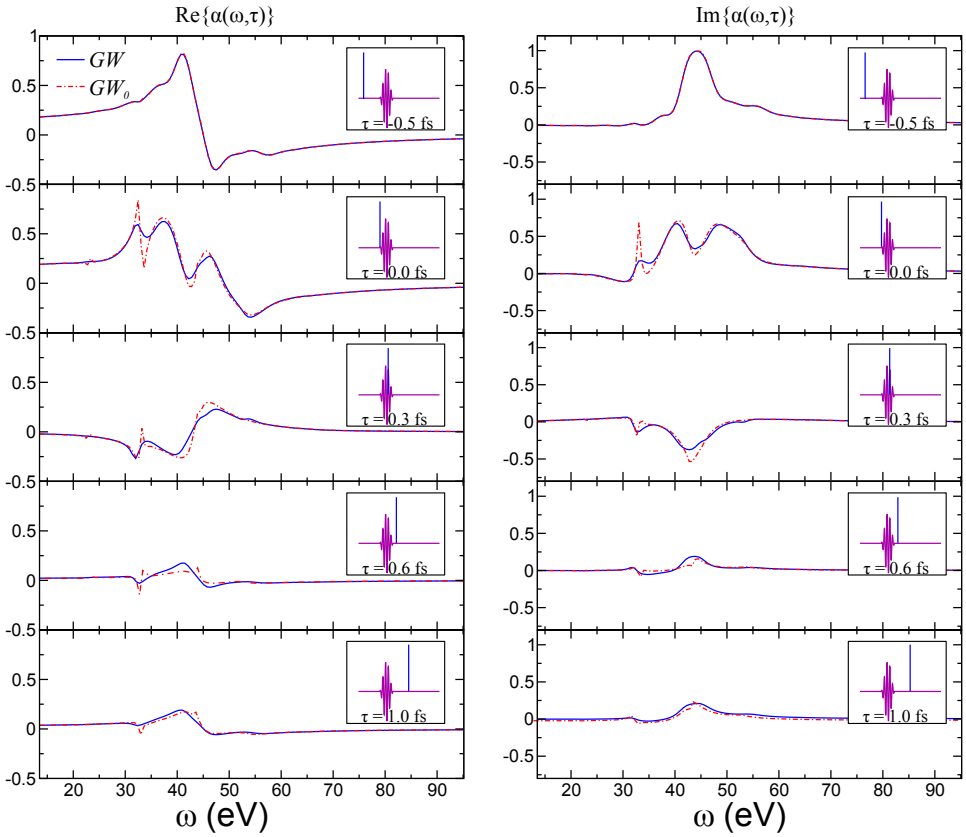

Figure 5. Transient refraction (left panel) and absorption (right) spectra for the GW (solid blue) and GW_0 (red dot-dashed line) approximation. The inset sketches the temporal arrangement of pump (amplitude $f_{p,0} = 0.3$ a. u.) and probe pulses.

presented the equations of motion for the two-times nonequilibrium Green's functions describing both the electronic and bosonic degrees of freedom. These equations were solved to determine the transient optical properties by simulating pump-probe setup. Our full propagation scheme yields, in contrast to the usual frozen-boson approach, accurate absorption spectra even in strong nonequilibrium situations.

Acknowledgments

This work is supported by the German Research Foundation (DFG) Collaborative Research Centre SFB 762 Functionality of Oxide Interfaces (Y. P.) and Grant Number PA 1698/1-1 (M. S. and Y. P.). We would like to thank Claudio Verdozzi, Andreas Wacker, Carl-Olof Almbladh for organizing this inspiring conference.

References

[1] Hüfner S 2003 *Photoelectron Spectroscopy: Principles and Applications* (Springer Science & Business Media)
[2] Uimonen A M, Stefanucci G and Leeuwen R v 2014 *J. Chem. Phys.* **140** 18A526
[3] Berakdar J and Kirschner J 2006 *Correlation Spectroscopy of Surfaces, Thin Films, and Nanostructures* (John Wiley & Sons)
[4] Schattke W and Hove M A V 2008 *Solid-State Photoemission and Related Methods: Theory and Experiment* (John Wiley & Sons)
[5] Pavlyukh Y, Schüler M and Berakdar J 2015 *Phys. Rev. B* **91** 155116
[6] Strinati G 1988 *Riv. Nuovo Cimento* **11** 1–86
[7] Stefanucci G and Leeuwen R v 2013 *Nonequilibrium Many-Body Theory of Quantum Systems: A Modern Introduction* (Cambridge University Press)

[8] Aryasetiawan F and Gunnarsson O 1998 *Rep. Prog. Phys.* **61** 237
[9] Strinati G, Mattausch H J and Hanke W 1982 *Phys. Rev. B* **25** 2867–2888
[10] Albrecht S, Reining L, Del Sole R and Onida G 1998 *Phys. Rev. Lett.* **80** 4510–4513
[11] Benedict L X, Shirley E L and Bohn R B 1998 *Phys. Rev. Lett.* **80** 4514–4517
[12] Rohlfing M and Louie S G 1998 *Phys. Rev. Lett.* **81** 2312–2315
[13] Onida G, Reining L and Rubio A 2002 *Rev. Mod. Phys.* **74** 601–659
[14] Pal G, Pavlyukh Y, Hübner W and Schneider H C 2011 *Eur. Phys. J. B* **79** 327–334
[15] Marques M A L, Maitra N T, Nogueira F M S, Gross E K U and Rubio A 2012 *Fundamentals of Time-Dependent Density Functional Theory* (Springer)
[16] Prodan E and Nordlander P 2002 *Chem. Phys. Lett.* **352** 140–146
[17] Prodan E and Nordlander P 2003 *Nano Lett.* **3** 543–547
[18] Sakko A, Rubio A, Hakala M and Hämaläinen K 2010 *J. Chem. Phys.* **133** 174111
[19] Schüler M, Berakdar J and Pavlyukh Y 2015 *Phys. Rev. A* **92** 021403
[20] Dahlen N E and van Leeuwen R 2007 *Phys. Rev. Lett.* **98** 153004
[21] Myöhänen P, Stan A, Stefanucci G and van Leeuwen R 2009 *Phys. Rev. B* **80** 115107
[22] Balzer K and Bonitz M 2012 *Nonequilibrium Green's Functions Approach to Inhomogeneous Systems* (Springer)
[23] von Friesen M P, Verdozzi C and Almbladh C O 2009 *Phys. Rev. Lett.* **103**
[24] Puig von Friesen M, Verdozzi C and Almbladh C O 2010 *Phys. Rev. B* **82** 155108
[25] Verdozzi C, Karlsson D, Puig von Friesen M, Almbladh C O and von Barth U 2011 *Chem. Phys.* **391** 37–49
[26] Kling M and Vrakking M 2008 *Annu. Rev. Phys. Chem.* **59** 463–492
[27] Krausz F and Ivanov M 2009 *Rev. Mod. Phys.* **81** 163–234
[28] Nagele S, Pazourek R, Feist J, Doblhoff-Dier K, Lemell C, Tőkési K and Burgdörfer J 2011 *J. Phys. B* **44** 081001
[29] Goulielmakis E, Loh Z H, Wirth A, Santra R, Rohringer N, Yakovlev V S, Zherebtsov S, Pfeifer T, Azzeer A M, Kling M F, Leone S R and Krausz F 2010 *Nature* **466** 739–743
[30] Lépine F, Sansone G and Vrakking M J J 2013 *Chem. Phys. Lett.* **578** 1–14
[31] Cavalieri A L, Müller N, Uphues T, Yakovlev V S, Baltuška A, Horvath B, Schmidt B, Blümel L, Holzwarth R, Hendel S, Drescher M, Kleineberg U, Echenique P M, Kienberger R, Krausz F and Heinzmann U 2007 *Nature* **449** 1029–1032
[32] Moskalenko A S, Pavlyukh Y and Berakdar J 2012 *Phys. Rev. A* **86** 013202
[33] Perfetto E, Uimonen A M, van Leeuwen R and Stefanucci G 2015 *Phys. Rev. A* **92** 033419
[34] Perfetto E, Sangalli D, Marini A and Stefanucci G 2015 *Phys. Rev. B* **92** 205304
[35] Lundqvist B I 1969 *Phys. Kondens. Mater.* **9** 236–248
[36] Langreth D C 1970 *Phys. Rev. B* **1** 471–477
[37] Minnhagen P 1975 *J. Phys. C* **8** 1535
[38] Mahan G D 2000 *Many-Particle Physics* (Springer Science & Business Media)
[39] Galperin M, Ratner M A and Nitzan A 2004 *Nano Lett.* **4** 1605–1611
[40] Dash L K, Ness H and Godby R W 2010 *J. Chem. Phys.* **132** 104113
[41] Ness H and Dash L K 2011 *Phys. Rev. B* **84** 235428
[42] White A J and Galperin M 2012 *Phys. Chem. Chem. Phys.* **14** 13809
[43] Gruebele M and Zewail A H 1993 *J. Chem. Phys.* **98** 883–902
[44] Zewail A H 2000 *J. Phys. Chem. A* **104** 5660–5694
[45] Schüler M, Pavlyukh Y and Berakdar J 2013 *J. Phys. Chem. Lett.* **4** 1131–1135
[46] Schüler M, Pavlyukh Y and Berakdar J 2014 *Phys. Rev. A* **89** 063421
[47] Boström E, Mikkelsen A and Verdozzi C 2015 *arXiv:1507.06975 [cond-mat, physics:physics]*
[48] Sentef M, Kemper A F, Moritz B, Freericks J K, Shen Z X and Devereaux T P 2013 *Physical Review X* **3** 041033
[49] Eckstein M and Werner P 2013 *Phys. Rev. Lett.* **110** 126401
[50] Dash L K, Ness H and Godby R W 2011 *Phys. Rev. B* **84**
[51] Säkkinen N, Peng Y, Appel H and Leeuwen R v 2015 *J. Chem. Phys.* **143** 234101
[52] Stan A, Dahlen N E and Leeuwen R v 2009 *J. Chem. Phys.* **130** 224101
[53] Lemell C, Neppl S, Wachter G, Tőkési K, Ernstorfer R, Feulner P, Kienberger R and Burgdörfer J 2015 *Phys. Rev. B* **91** 241101
[54] Canney S A, Sashin V A, Ford M J and Kheifets A S 1999 *Journal of Physics: Condensed Matter* **11** 7507
[55] Giuliani G and Vignale G 2005 *Quantum Theory of the Electron Liquid* (Cambridge University Press)